Hydrodynamic Simulation of Suspended Solids Concentration in Isahaya Regulating Reservoir

Cong Khiem Ta[1], Seiji Suzuki[1], and Nhat Huy Nguyen[2*]

[1]Department of Advanced Engineering, Graduate School of Engineering, Nagasaki University, 1-14 Bunkyo, Nagasaki, 852-8521 Japan

[2]Faculty of Environment and Natural Resources, Ho Chi Minh City University of Technology, VNU-HCM, 268 Ly Thuong Kiet St., Dist. 10, Ho Chi Minh City, Vietnam

ARTICLE INFO

Received: 3 Sep 2019
Received in revised: 16 Jan 2020
Accepted: 13 Feb 2020
Published online: 11 Mar 2020
DOI: 10.32526/ennrj.18.2.2020.20

Keywords:
Suspended solids (SS)/ Isahaya regulating reservoir/ Osaka daigaku estuary model (ODEM)/ Unmanned Aerial Vehicle (UAV)

*** Corresponding author:**
E-mail: nnhuy@hcmut.edu.vn

ABSTRACT

In this study, Osaka daigaku estuary model (ODEM) was applied for hydrodynamic simulation of suspended solids (SS) concentration in the Isahaya regulating reservoir. Water samples were collected every hour from 9:00 to 15:00 at nine sampling points inside the observation area of the reservoir. Parameters used for the model included initial conditions (i.e., SS concentration, water depth, temperature, and salinity) and boundary conditions (i.e., wind speed and direction, atmospheric temperature, solar irradiation, and cloud cover). The calculated results of SS in the reservoir and its concentration fluctuation from the model were compared with those estimated from the image analysis of unmanned aerial vehicle (UAV) and observed results. The SS simulated from ODEM distributed in high concentration, whereas that estimated from UAV distributed in low concentration although in both data they spread across a wide range at most investigated times. Although there was a big difference between the accuracy of ODEM and UAV, the SS concentration values described by them were closed to the observed values. Between them, the ODEM model showed its advantages in simulating the SS concentration and achieved more accuracy than UAV, showing a potential for using ODEM model in monitoring of SS in water.

1. INTRODUCTION

There have been hydraulic, ecological, and biological changes to water quality in Isahaya regulating reservoir since the Isahaya Bay witnessed the erection of a sea dike in 1997. Among these changes, it is notable that SS is one of the main factors that has a great influence on water quality and have been investigated by scientists over the years (Bilotta and Brazier, 2008; Chebbo and Bachoc, 1992; Gartner, 2004). Methods for observing SS in water environment are primarily based on conventional methods (e.g., field sampling and then analysis in laboratory). These methods are often time-consuming, labor-intensive, and costly but not well representative of the large observing area, which are unlikely to meet the long-term observing requirements and can result in failure to realize the quick fluctuations of water quality over time (Schaeffer et al., 2013). On the contrary, together with the strong development of information technology and electrical telecommunications in recent years, many programs and computer software have been developed and widely applied in many fields of study, such as Fortran programming language. Osaka daigaku estuary model (ODEM) based on Fortran 90 program statements was built and can be considered as a means of remote simulation of SS. This model is composed of elements of a numerical model regarding the process of fluid dynamics described by basic hydrodynamic equations such as the three-dimensional partial differential equations of flow motion, flow continuity, heat, salt transport, and water density. In addition, it can be used to observe water environment through simulating SS besides other water quality parameters in different places on a large scale of a target area and over a long period of time thanks to its ease of operation and portability. ODEM have been used to simulate seasonal tidal residual

Citation: Ta CK, Suzuki S, Nguyen NH. Hydrodynamic simulation of suspended solids concentration in Isahaya regulating reservoir. Environ. Nat. Resour. J. 2020; 18(2): 209-223. DOI: 10.32526/ennrj.18.2.2020.20

current in Bohai Sea and the modelled tidal residual current was discovered to be weak in most parts of the Bohai Sea but much more powerful in the inshore parts. Similarly, it was apparent from the central part of the Bohai Sea that seasonal wind had a considerable influence on the tidal residual current, though it had insignificant effect on the tidal residual current in the inshore part of the Bohai Sea (Liang et al., 2003a; Liang et al., 2003b). The model was also applied for converting model parameters, in which the temporal-spatial conversion approach was revealed to be better than others (i.e., temporal, spatial, and non-temporal and non-spatial) (Li et al., 2012). However, SS concentration was not considered in those studies.

The interaction between SS and water quality parameters such as biochemical oxygen demand (BOD), salinity, and phosphorus has been studied and analyzed, while there have been a lack of specific SS observing methods. For example, several studies have been done on the effect of SS on the reservoir water quality due to salinity reduction (Sasaki, 2017) and the effect of SS changes on BOD after construction of a sea dike in Isahaya bay (Nishida et al., 1997). There were also works on the analysis of SS behavior according to the increase of seawater from the Ariake Sea (Nagase et al., 2014), the resuspension of SS caused by the coagulation of phosphorus in Isahaya reservoir (Mitsugi et al., 2013), and the settling velocity of SS affected by seawater from Ariake Sea flowing to Isahaya reservoir (Koga et al., 2003). Furthermore, SS concentration has been estimated by using other methods such as Acoustic Doppler Current Profiler (ADCP, using echo intensity backscattered from SS) (Dwinovantyo et al., 2017), Landsat 7 (using Landsat 7 as remote sensing) (Shahzad et al., 2018), and online auto sensors (using high frequency observation with online auto sensors) (Valkama and Ruth, 2017). Although it is worthy to investigate, up to the present, there have not been any works on the usage of ODEM for simulation of SS in Isahaya regulating reservoir.

In this work, we aimed to apply computational simulation through the ODEM model to predicting the SS concentration which dominates water quality and ecosystem in Isahaya regulating reservoir. The simulated results were then compared with those estimated from unmanned aerial vehicle (UAV) and field sampling to elucidate the capability of ODEM model in simulating SS in the reservoir. Besides, consideration of crucial relationships between biomass development of microorganism and pollutant concentration was also discussed in this work.

2. METHODOLOGY

2.1 Instruments and equipment for field sampling, measuring, and analyzing

Items required for field sampling, measuring, and analyzing include a van, inflatable pontoon, plastic bottle, wash bottle, DR/2010 portable datalogging spectrophotometer, laboratory tissue, AAQ1183-H multi-parameter water quality meter, Neo pyranometer, and WJ-24 hand anemoscope/ anemometer. The detailed technical specifications of DR/2010 portable datalogging spectrophotometer are described in Table S2.

2.2 Study area

A large-scale sea dike project with a length of 7 km (Yamaguchi and Hayami, 2018) along with a reclamation project were constructed in 1997 (Mitsugi et al., 2013) to protect Isahaya city from saline intrusion and high tidal waves (Figure 1). Therefore, the sea dike has incidentally created a large regulating reservoir situated between the residential area and the dike to the southwest of the Ariake Sea. The reservoir covers an area of 2,600 ha, comprising 13 rivers starting from the first class Honmyo River, which has a depth of 3.5 m at the deepest part and an average depth of about 1.1 m (Yamaguchi and Hayami, 2018). This regulating reservoir, therefore, has a relatively shallow area of water and the bottom sludge is easily disturbed by wind. Besides, the hydraulic, ecological, and biological characteristics of the reservoir have been changed, such as eutrophication due to increase of phosphorus from contaminant loads in the flood influent (Niki et al., 1999), tidal current high, decline in salinity, increase in suspended solids (SS), and oxygen depletion on account of the discharge of rainwater and domestic wastewater. Particularly, the outbreak of red tide has become a phenomenon expressing degradation of water quality in the reservoir during the winter between 2000 and 2001 (Tada et al., 2010).

2.3 Sampling points

The position of sampling points is shown in Figure 2 whereby the sampling points were marked on the picture according to the actual coordinates. These points were chosen in the observation area near the bank beside the north floodgate of the sea dike.

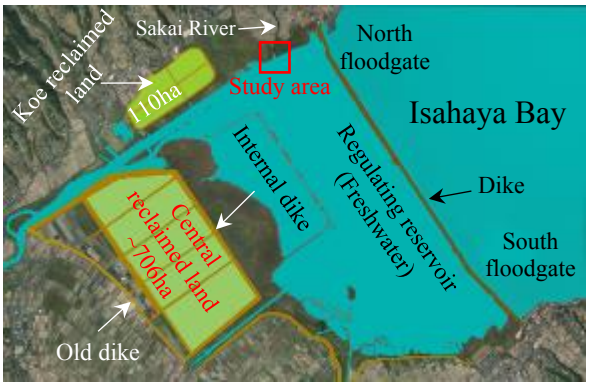

Figure 1. Study area in Isahaya regulating reservoir

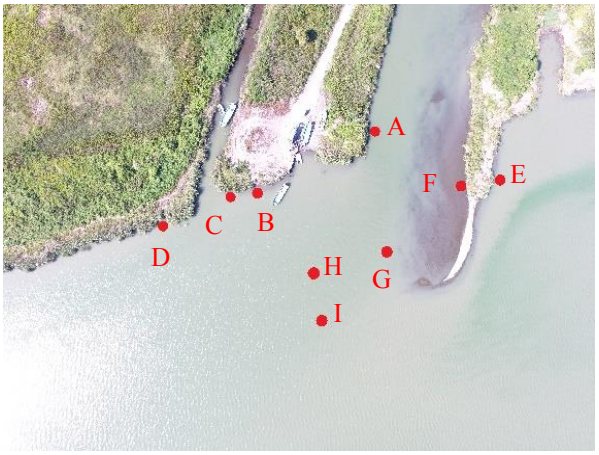

Figure 2. Positions of sampling points in study area

2.4 Sampling and measurement procedures

Sampling is one of the important steps in the operation of the model and the results from the analysis and measurement are the important database for the model. The values of the SS analysis results by the spectrophotometer at the first measurement are the baseline in which the simulation results of the model at the next measurement are based on. The principle of this method is to measure the transmittance of light passing through a solution containing SS. On the other hand, this transmittance is proportional to the absorbance in relation: A=-logT, and the absorbance is proportional to the concentration of SS absorbed (Harris, 2007). According to Krawczyk and Gonglewski (1959), SS concentration in the sewage samples after being diluted with city water was directly proportional to the transmittance. Further, this method was consistent with the law of colorimetry and can be applied for measuring SS concentration.

2.5 Assigning the initial values of SS concentration

Assuming that the sequence number of cells on the horizontal and vertical direction are known, two lines are drawn through the two cells. If the intersection of the two lines coincides with one of the sampling points (e.g., point A Figure 2), the initial value of the SS concentration at that point is the initial value of the SS concentration at the point A. Otherwise, it is the initial value of the SS concentration at adjacent sampling point (e.g., point B in Figure 2).

2.6 Assigning the initial values of water depth, water temperature, and salinity

The values of water depth, water temperature, and salinity were constant at different sampling points where the water temperature and salinity were taken as 10 m and 0 ‰, respectively, and the water depths at all points were 0.5 m.

2.7 Entering meteorological data as input parameters into the model

Meteorological parameters were also measured during sampling including wind speed, wind direction, air temperature, radiation, total solar radiation, and cloud cover as shown in Table 1.

Table 1. Meteorological data used as input parameters for the model

Time	Air temperature (°C)	Wind		Total solar radiation (MJ/m^2)	Cloud cover
		Speed (m/s)	Direction (degree)		
09:00	22.9	0.1	135	1.49	0+
10:00	24.0	0.0	0	1.82	
11:00	26.5	1.0	135	2.11	
12:00	27.1	3.1	90	2.65	6
13:00	28.2	3.1	135	2.93	
14:00	28.3	2.3	90	2.73	
15:00	28.5	2.8	90	2.03	7

2.8 Mass balance formula of SS

The sediment particles can be supplied directly into the flowing water from the sweeping layer or bottom. In the actual watershed, the transition process is complicated because sediment is not a single-sized particle and the flow is locally changing. As a method for evaluating the rolling up flux of sediment particles, sediment is considered as one of continuous and granular particles. In this study, it is assumed that the size of sediment particles in Isahaya regulating reservoir is 4 μm (Nishida et al., 2014) and after leaving the bottom it immediately transits to a floating state. Furthermore, if the sweeping force exceeds its limit, rolling up occurs and it is evaluated by Equation 1. The sweeping force is displayed in a dimensionless manner as $\left(\frac{\tau_b}{\sigma-\rho}g\cdot d\right)$.

$$\begin{cases} \tau_{*f} \le \tau_{*cf} & F_c = 0 \\ \tau_{*f} > \tau_{*cf} & F_c = \sigma v_s P_s / a_s \end{cases} \quad (1)$$

Where; τ_{*cf} and τ_{*f} are dimensionless sweeping force and its value at the movement limit, respectively; ρ is density of water (kg/m^3); σ and v_s are density (kg/m^3) and volume (m^3) of the sediment particle, respectively; a_s is orthogonal projection area of the sediment particle (m^2); and p_s is pick-up rate.

The pick-up rate is evaluated by the following equation (Murakami et al., 1992):

$$\frac{\sqrt{P_S}}{\sqrt{\left(\frac{\sigma}{\rho-1}\right)\frac{g}{d}}} = F_P\cdot\tau_{*f}\cdot\left(1-k_2\frac{\tau_{*cf}}{\tau_{*f}}\right)^2 \quad (2)$$

In addition, τ_{*cf} is calculated from the equation below:

$$\tau_{*f} = \frac{\mu}{1+k_L\mu}\cdot\frac{1}{\varepsilon\cdot A_*^2\cdot C_D A_2/2A_3} \quad (3)$$

Where; d is diameter of the sediment particle (m); g is gravitational acceleration (m/s^2); k_L is drag/lift ratio (0.85); μ is static friction coefficient (1.0); A_2 and A_3 are shape factors of the sediment particle; C_D is drag coefficient when the Reynolds number is large enough, C_D=0.4, F_p=0.03, k_2=0.7, m=2.89.

Sediment flux is amount corresponding to the settling velocity to the bottom (kg/ (m^2·s)):

$$Fd = SS\cdot w_0 \quad (4)$$

Where; W_0 is the settling velocity of SS in freshwater (m/s). Settling velocity is evaluated by Rubey's equation shown in the following equation:

$$\frac{w_0}{\sqrt{\left(\frac{\sigma}{\rho}-1\right)gd}} = \sqrt{\frac{2}{3}+\frac{36v^2}{\left(\frac{\sigma}{\rho}-1\right)gd^3}}-\sqrt{\frac{36v^2}{\left(\frac{\sigma}{\rho}-1\right)gd^3}} \quad (5)$$

2.9 Calculation conditions of model

The model uses the target calculation area as shown in Figure 2. The spatial difference interval is Δx=Δy=10 m in horizontal direction and 10 layers divided into four kinds of thickness Δz in vertical direction including 5 layers of 0.5 m, 1 layer of 0.4 m, 1 layer of 0.3 m, and 3 layers of 0.1 m from bottom to surface. The time difference interval was Δt=0.1 s. The boundary conditions (i.e., wind speed, wind direction, air temperature, radiation, and cloud cover) were taken from field sampling in Table 1. The initial conditions such as SS concentration, water depth, water temperature, and salinity at each sampling point were applied to the reservoir (Sections 2.5-2.7).

3. RESULTS AND DISCUSSION

3.1 Analysis results of SS concentration

Figure 3 plots the changes in SS concentration from 9:00 to 15:00 as sampled and analyzed on September 28, 2018. In general, the SS concentration at sampling points decreased with time except at points F and H. During the period from 9:00 to 15:00, SS concentration at points E and I increased significantly from 9:00 to 12:00 and followed by a considerable fluctuation from 12:00 to 15:00. To be more precise, SS concentration at these points E and I declined dramatically from 124 and 155 mg/L at 12:00 to 40 and 114 mg/L at 13:00, respectively, but later went up sharply by 67 and 34 mg/L, respectively, at 14:00. This could come from anthropogenic activities that occurred between two periods of time before and after 13:00 in the area. At the same time, SS concentration at points A, F, G, and H went up marginally and always lower in comparison with that at points E and I. During the same period, there was an opposite tendency of SS concentration at points B, C, and D. The period starting from 12:00 onwards experienced a downward trend of SS concentration at most points except F and H. However, most of the SS concentration at the sampling points was very high, in which the SS concentrations at points E and I were the highest ones. In other words, p value (0.001) in Table 2 was less than 0.05 (significant level), i.e., variances

between observed SS at 9 points were heterogeneous. It was not surprising, therefore, that ANOVA cannot be used on this account. Despite this, a post-hoc test (Table 3) needs to be used to identify further which pairs of points are statistically higher or lower. The mean observed SS at points A and B was statistically different because p equal to 0.001 was less than 0.05. The mean observed SS at point A was less than that at point B because the mean difference in observed SS between these two points was negative when the mean observed SS at point B was subtracted from mean observed SS at point A. Similarly, the mean observed SS between the following pairs also were statistically significant, including A:C, A:D, A:E, A:G, A:H, A:I, B:F, B:I, C:F, C:I, D:F, E:F, E:G, F:H, F:I, G:H, G:I, and H:I in which the mean differences with negative values were found in the following pairs: A:C, A:D, A:E, A:G, A:H, A:I, B:I, C:I, F:H, F:I, G:H, G:I, and H:I. Pairs with p values less than 0.05 that are not listed above were those whose mean differences had values with the sign inverse to that of the mean differences in the above pairs, including B:A, C:A, D:A, E:A, G:A, H:A, I:A, F:B, I:B, F:C, I:C, F:D, F:E, G:E, H:E, I:F, H:G, I:G, and I:H. Among the pairs whose mean differences had statistically significant values of negative and positive signs, pairs E:G and G:E had the highest statistically significant mean differences with p values equal to 0.027 compared to those of the others. Pairs A:H, A:I, F:H, F:I, H:A, H:F, I:A, and I:F, meanwhile, were those whose mean differences were the lowest statistically significant because their p values were equal to 0.000. The very high SS concentration at most sampling points suggests that water quality at reservoir is low due to high turbidity, water layers disturbed by wind, and development of microbiological biomass (Mitsugi et al., 2013). This was contrast to the lowest SS concentration at point A where the water was clearest due to its lowest turbidity. Indeed, from the correlation coefficient in Table 4, it is apparent that three water quality parameters, consisting of turbidity, temperature, and chlorophyll in which chlorophyll is representative of microbiological biomass, exerted a certain influence on observed SS, especially at point G for turbidity, F for temperature, and points C and G for chlorophyll where relative correlations with observed SS were seen clearly. Besides having good correlations with observed SS at the above points, turbidity and temperature were also correlated with observed SS with moderate correlation coefficients of over 0.5 to just below 0.8 which could be taken into account such as 0.64 at point B and 0.57 at point C for turbidity; and 0.53 at point C, 0.74 at point D, and 0.58 at point H for temperature. Also, despite of having no moderate correlation coefficients with observed SS, chlorophyll had two correlation coefficients of over 0.8 compared to the other two parameters. Therefore, it can be said that high turbidity, temperature, and chlorophyll were associated with high SS concentration.

Table 2. Test of homogeneity of variances between observed SS concentrations at sampling points

Levene statistic	df1	df2	Sig.
3.772	8	54	0.001

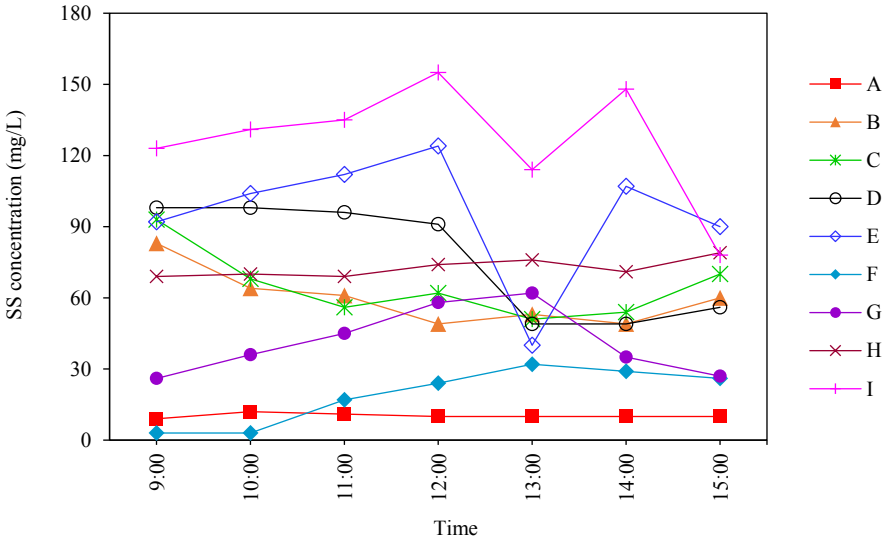

Figure 3. SS concentration fluctuation at sampling points

Table 3. Dunnett T3 test for multiple comparisons between observed SS of point pairs

(I) Point	(J) Point	Mean difference (I-J)	Std. error	Sig.	95% Confidence interval	
					Lower bound	Upper bound
A	B	-49.57143*	4.47822	**0.001**	-71.1067	-28.0362
	C	-54.57143*	5.41226	**0.001**	-80.6400	-28.5028
	D	-66.42857*	9.06702	**0.006**	-110.1987	-22.6584
	E	-85.28571*	10.25525	**0.003**	-134.8054	-35.7661
	F	-8.85714	4.53632	0.771	-30.6746	12.9604
	G	-31.00000*	5.41791	**0.022**	-57.0960	-4.9040
	H	-62.28571*	1.50509	**0.000**	-69.2554	-55.3160
	I	-116.00000*	9.62741	**0.000**	-162.4819	-69.5181
B	A	49.57143*	4.47822	**0.001**	28.0362	71.1067
	C	-5.00000	7.00631	1.000	-32.8827	22.8827
	D	-16.85714	10.09984	0.909	-59.9003	26.1860
	E	-35.71429	11.17882	0.215	-84.2552	12.8266
	F	40.71429*	6.35407	**0.001**	15.6102	65.8184
	G	18.57143	7.01068	0.383	-9.3309	46.4737
	H	-12.71429	4.69694	0.397	-33.8872	8.4587
	I	-66.42857*	10.60580	**0.005**	-112.0471	-20.8101
C	A	54.57143*	5.41226	**0.001**	28.5028	80.6400
	B	5.00000	7.00631	1.000	-22.8827	32.8827
	D	-11.85714	10.54727	0.998	-55.5035	31.7892
	E	-30.71429	11.58465	0.401	-79.5718	18.1432
	F	45.71429*	7.04360	**0.001**	17.7095	73.7191
	G	23.57143	7.64119	0.203	-6.6169	53.7597
	H	-7.71429	5.59458	0.973	-33.4197	17.9911
	I	-61.42857*	11.03273	**0.008**	-107.5034	-15.3537
D	A	66.42857*	9.06702	**0.006**	22.6584	110.1987
	B	16.85714	10.09984	0.909	-26.1860	59.9003
	C	11.85714	10.54727	0.998	-31.7892	55.5035
	E	-18.85714	13.67927	0.985	-73.0682	35.3539
	F	57.57143*	10.12574	**0.008**	14.5047	100.6381
	G	35.42857	10.55017	0.154	-8.2230	79.0801
	H	4.14286	9.17702	1.000	-39.3502	47.6359
	I	-49.57143	13.21512	0.070	-101.8196	2.6768
E	A	85.28571*	10.25525	**0.003**	35.7661	134.8054
	B	35.71429	11.17882	0.215	-12.8266	84.2552
	C	30.71429	11.58465	0.401	-18.1432	79.5718
	D	18.85714	13.67927	0.985	-35.3539	73.0682
	F	76.42857*	11.20222	**0.003**	27.8792	124.9779
	G	54.28571*	11.58729	**0.027**	5.4251	103.1464
	H	23.00000	10.35263	0.636	-26.2676	72.2676
	I	-30.71429	14.05698	0.651	-86.2954	24.8668
F	A	8.85714	4.53632	0.771	-12.9604	30.6746
	B	-40.71429*	6.35407	**0.001**	-65.8184	-15.6102
	C	-45.71429*	7.04360	**0.001**	-73.7191	-17.7095
	D	-57.57143*	10.12574	**0.008**	-100.6381	-14.5047
	E	-76.42857*	11.20222	**0.003**	-124.9779	-27.8792
	G	-22.14286	7.04794	0.189	-50.1670	5.8812

Table 3. Dunnett T3 test for multiple comparisons between observed SS of point pairs (cont.)

(I) Point	(J) Point	Mean difference (I-J)	Std. error	Sig.	95% Confidence interval	
					Lower bound	Upper bound
	H	-53.42857*	4.75237	**0.000**	-74.8826	-31.9746
	I	-107.14286*	10.63047	**0.000**	-152.7771	-61.5086
G	A	31.00000*	5.41791	**0.022**	4.9040	57.0960
	B	-18.57143	7.01068	0.383	-46.4737	9.3309
	C	-23.57143	7.64119	0.203	-53.7597	6.6169
	D	-35.42857	10.55017	0.154	-79.0801	8.2230
	E	-54.28571*	11.58729	**0.027**	-103.1464	-5.4251
	F	22.14286	7.04794	0.189	-5.8812	50.1670
	H	-31.28571*	5.60005	**0.018**	-57.0186	-5.5528
	I	-85.00000*	11.03550	**0.001**	-131.0790	-38.9210
H	A	62.28571*	1.50509	**0.000**	55.3160	69.2554
	B	12.71429	4.69694	0.397	-8.4587	33.8872
	C	7.71429	5.59458	0.973	-17.9911	33.4197
	D	-4.14286	9.17702	1.000	-47.6359	39.3502
	E	-23.00000	10.35263	0.636	-72.2676	26.2676
	F	53.42857*	4.75237	**0.000**	31.9746	74.8826
	G	31.28571*	5.60005	**0.018**	5.5528	57.0186
	I	-53.71429*	9.73108	**0.024**	-99.9314	-7.4972
I	A	116.00000*	9.62741	**0.000**	69.5181	162.4819
	B	66.42857*	10.60580	**0.005**	20.8101	112.0471
	C	61.42857*	11.03273	**0.008**	15.3537	107.5034
	D	49.57143	13.21512	0.070	-2.6768	101.8196
	E	30.71429	14.05698	0.651	-24.8668	86.2954
	F	107.14286*	10.63047	**0.000**	61.5086	152.7771
	G	85.00000*	11.03550	**0.001**	38.9210	131.0790
	H	53.71429*	9.73108	**0.024**	7.4972	99.9314

* The mean difference is significant at the 0.05 level.

Table 4. Correlation coefficient of water quality parameters with observed SS (R^2)

Point	Turbidity	pH	DO	Temperature	Chlorophyll	Salinity
A	0.0125	0.3410	0.0509	0.0282	0.0918	0.7091
B	0.6352	0.0771	0.3185	0.4691	0.4897	0.6326
C	0.5701	0.0617	0.0654	0.5300	**0.8311**	**0.9297**
D	0.2897	0.2417	0.6365	0.7420	0.4528	0.1528
E	0.1268	0.0257	0.0779	0.0713	0.0237	0.0176
F	0.1458	0.0295	0.3183	**0.8579**	0.4590	0.0000
G	**0.9722**	0.0281	0.3108	0.0715	**0.8973**	0.6108
H	0.3199	0.5444	0.6181	0.5849	0.2804	0.0000
I	0.3963	0.1651	0.0085	0.1673	0.0042	0.6798

3.2 Distribution of SS concentration and flow structure in observation area

In a previous study of Dohi in our group (unpublished results), SS concentration in Isahaya Bay was also observed and estimated from photos taken by UAV. Therefore, in order to understand objectively hydrodynamic simulation of SS concentration utilizing the model, the results in this study were compared with those in the above study. The ODEM model was operated according to the initial conditions and boundary conditions described in Sections 2.5-2.7. The obtained results were

exported as plots showing the distribution of SS concentration and flow structure.

As displayed in Figure 4, it is obvious that SS distributed in low concentration through the vicinity of Sakai River (Figure 1). SS distributed in high concentration in the remote area of the estuary where E and I points were situated. Thus, this result conformed to the field analysis results at points E and I as shown in Section 3.1. However, there was little difference between results estimated from the UAV and those simulated from ODEM. Whereas simulated SS (on the left) distributed in high concentration, the estimated SS (on the right) distributed in slightly low concentration although both of them spread across a large range at most hours from 9:00 to 15:00. In particular, the results obtained from image analysis on the right in the area around the estuary from 12:00 onwards showed that SS distributed in low concentration. It is explained that the low concentration of SS in surroundings of the estuary is due to clear water flowing from the Sakai River into the reservoir with low flowrate as well as the low wind speed in this area.

In contrast, SS distributed in high concentration in the remote area of the estuary at most investigated times could be because of (i) low salinity in the reservoir (Table S3), (ii) large reservoir area, (iii) increase in wind speed over time, and (iv) increase in stratification. Regarding salinity, there are always two types of ions (Na^+ and Cl^-) of the sodium chloride compound in seawater. Once these two types of ions encounter solid particles such as clay particles, suspended solids, and suspended sediments, the phenomenon of combining ions to form molecules (also called combination reaction) will take place thereafter. At that point, the negative ions of the particles will be neutralized by positive ions of salt in the seawater then the particles will be combined together and form larger particles (Sasaki, 2017). Once formed large enough, these particles will overcome the repulsive force of water and sink into the reservoir. By this way, the more seawater there is, the less suspended solids there are and vice versa. Also, the vertical diffusion will decrease with the higher salinity (Kim et al., 2018), and the suspended particles will be easier to settle. Moreover, with a large area of 2,600 ha, Isahaya regulating reservoir has a high wind disturbance resulting from its large surface momentum (Magee and Wu, 2017) combined with low water depths, the bottom sludge or sediment is easily disturbed by wind. Furthermore, the increase in wind speed over time (Table 1) could also have a significant effect. Bottom sludge or sediment disturbed by high wind speed will make water turbid. Finally, an increase in water temperature (Table S3) leads to increased stratification. Once stratification takes place, the water convection of internal and external parts in the reservoir will occur simultaneously. Water of the internal part flows outward in the upper layer in contrast to that in the lower layer (Sasaki, 2017). Therefore, the water layers will be disturbed along with the circulation of water in the reservoir. Since the sea dike was built, areas, containing water in the reservoir, have become closed areas and can undergo eutrophication under hypoxic conditions (Hodoki and Murakami, 2006). Water quality in such areas is then deteriorated due to increased amount of bottom sludge or sediment generated from algae and aquatic plants, which results in increased concentration of SS. In theoretical terms, this result could be explained in this way, but the fact (Table 5) remains that salinity and water temperature had statistically significant linear relationships with observed SS ($p<0.01$) as against correlation between wind speed and observed SS. Moreover, water temperature and observed SS was negatively correlated ($r=-0.33$), meaning that greater water temperature related to smaller amount of observed SS or vice versa. This could be attributed to the sample size of salinity was different to that of the other two parameters because of missing measured values of salinity at point F. Considering only 56 observations at point F, salinity was closely correlated with observed SS, but the direction of relationship was negative. However, if a full 63 (7 times × 9 points) observations had been made, the correlation would have remained the same, but the direction of the relationship would have been positive. In addition, it was the first attempt to apply ODEM for modelling SS concentration and the analysis of SS was mistakenly not repeated, which contributed to the limitation of this study. Briefly, the results obtained from ODEM, from which SS distributed in low concentration around the estuary, were closer to the field analysis results than that from UAV.

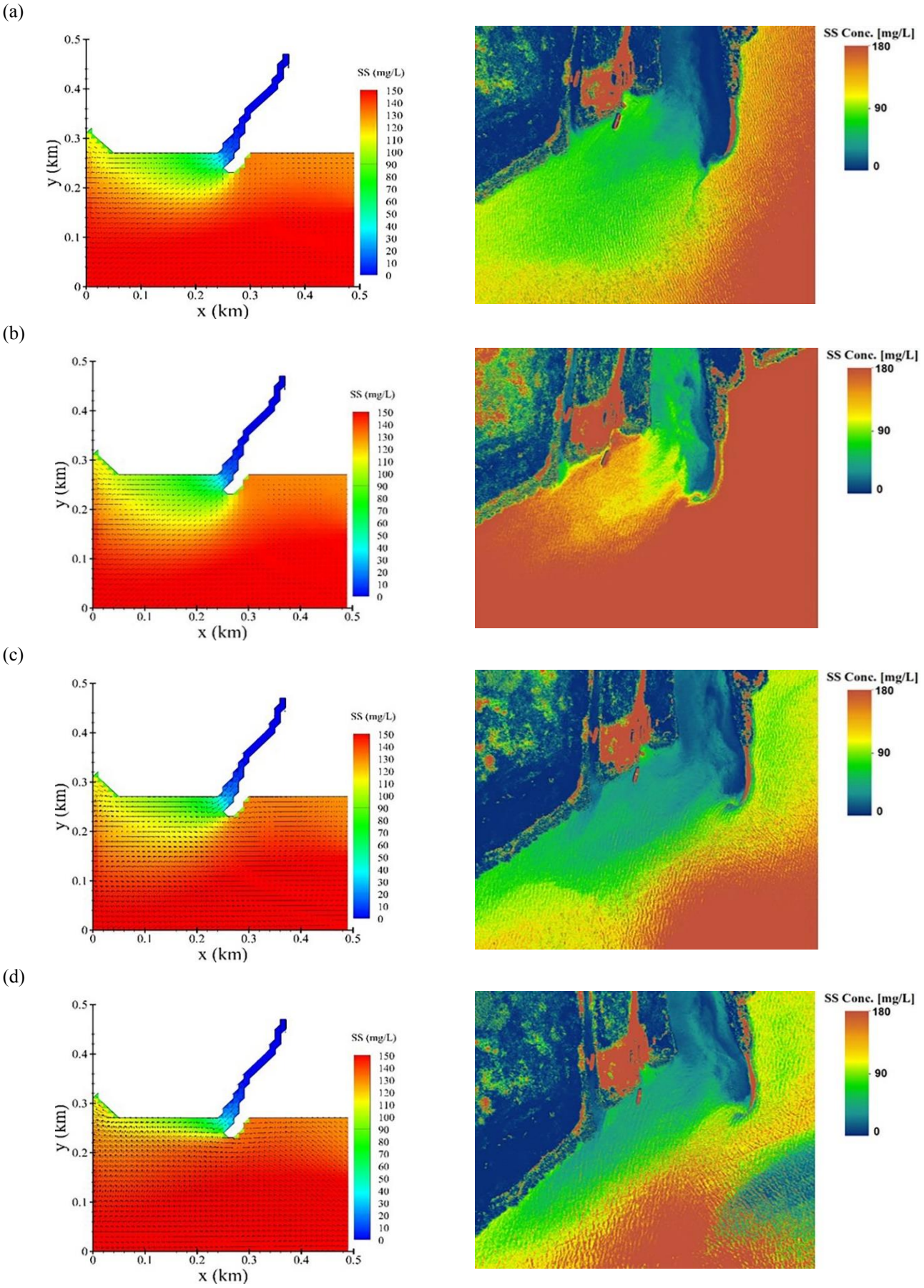

Figure 4. Distribution of SS concentration and flow structure obtained from ODEM (left) and UAV (right) at (a) 9:00, (b) 10:00, (c) 11:00, (d) 12:00, (e) 13:00, 14:00, and (g) 15:00

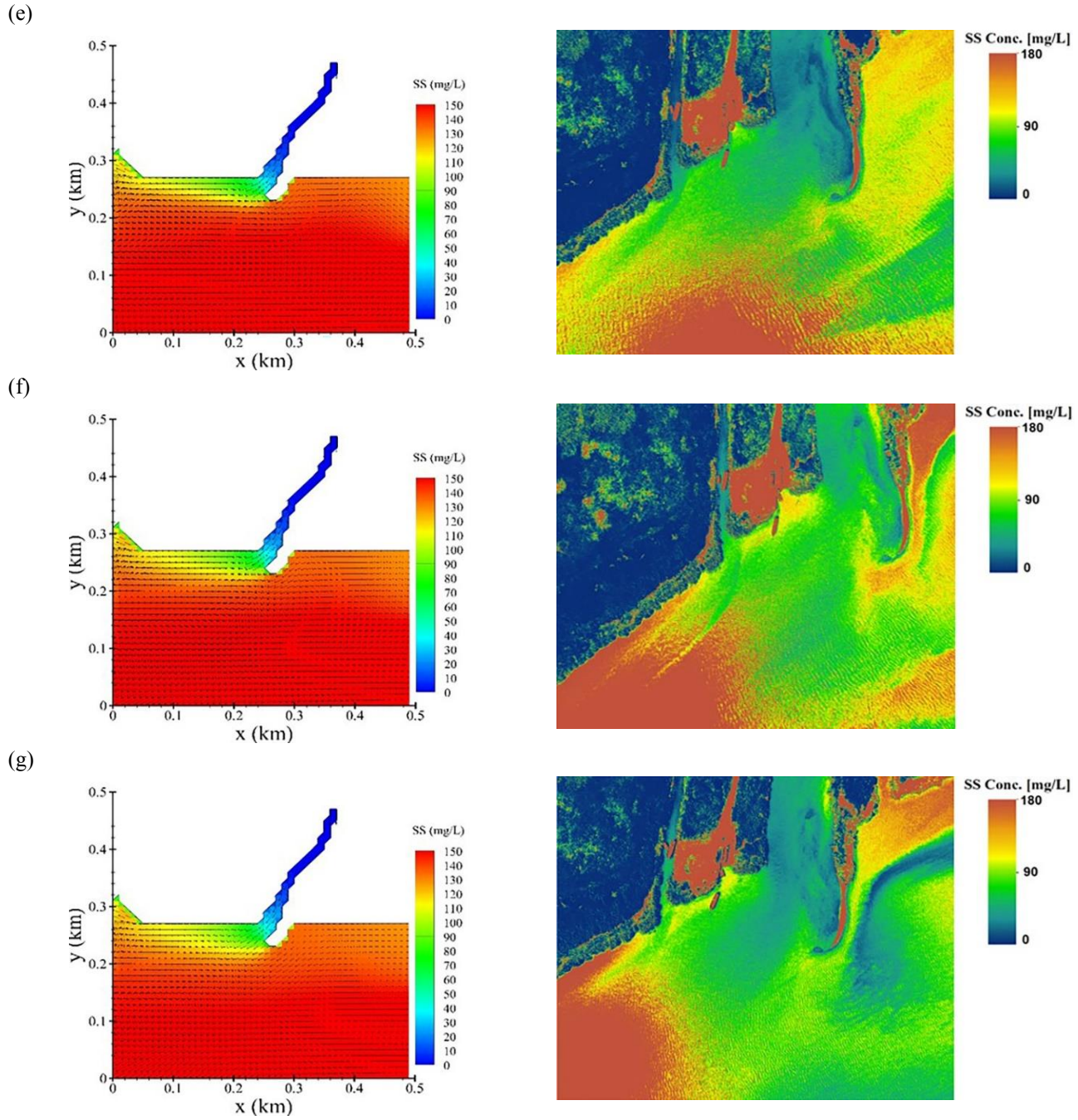

Figure 4. Distribution of SS concentration and flow structure obtained from ODEM (left) and UAV (right) at (a) 9:00, (b) 10:00, (c) 11:00, (d) 12:00, (e) 13:00, 14:00, and (g) 15:00 (cont.)

Table 5. Correlation matrix of water quality parameters and meteorological parameters with observed SS

		Observed SS	Salinity	Wind speed	Water temperature
Observed SS	Pearson Correlation	1	0.412**	-0.063	-0.330**
	Sig. (2-tailed)	-	0.002	0.626	0.008
	N	63	56	63	63
Salinity	Pearson Correlation	0.412**	1	-0.220	-0.149
	Sig. (2-tailed)	0.002	-	0.103	0.273
	N	56	56	56	56

Table 5. Correlation matrix of water quality parameters and meteorological parameters with observed SS (cont.)

		Observed SS	Salinity	Wind speed	Water temperature
Wind speed	Pearson correlation	-0.063	-0.220	1	0.719**
	Sig. (2-tailed)	0.626	0.103		0.000
	N	63	56	63	63
Water temperature	Pearson Correlation	-0.330**	-0.149	0.719**	1
	Sig. (2-tailed)0	0.008	0.273	0.000	
	N	63	56	63	63

** Correlation is significant at the 0.01 level (2-tailed).

3.3 Comparison of SS concentration simulated from ODEM and estimated from UAV with observed values

The comparison of simulated values from ODEM, the estimated values from the UAV, and the observed values from field sampling are presented in Table 6 (processed from detailed data of Table S4) and Figure 5. In short, Table 6 summarizes the errors between the SS concentration values from ODEM and UAV and the observed results. It can be seen that the errors at point F of both ODEM and UAV were very high as opposed to other points. These high errors could have resulted from differences in water depth between this point and other points. During the sampling period, water parameters were analyzed manually in situ, consisting of turbidity, pH, DO, temperature, chlorophyll, and salinity in which water temperature and salinity were the main factors directly affecting results of the model because these two parameters were two of three parameters (water depth, water temperature, and salinity) used as the initial values of the model (Section 2.6). Therefore, errors were unavoidable because the sampling depth of each point at different times along with movement of hands could have been different. Based on the study of Dwinovantyo et al. (2017), only an error of 5% between SS concentrations from ADCP and field analysis was detected. By comparison, this (high error at point F) declared that the ODEM and UAV did not have a high level of ability to simulate and estimate SS concentration, respectively.

Table 6. Error between the SS concentration values from ODEM and UAV and the observed results

Time	Error between SS concentration values from ODEM and observed results (%)								
	A	B	C	D	E	F	G	H	I
09:00	34	45	36	24	44	393	0	14	19
10:00	13	25	11	24	26	483	20	12	27
11:00	42	9	23	15	17	45	22	3	16
12:00	93	11	7	12	7	23	29	27	12
13:00	102	14	43	73	236	11	35	9	21
14:00	135	36	49	90	26	14	28	20	9
15:00	174	12	16	69	50	26	70	3	63
Time	Error between SS concentration values from UAV and observed results (%)								
09:00	52	12	43	56	3	15	55	20	11
10:00	6	5	12	34	14	390	13	15	26
11:00	25	1	12	58	6	49	14	10	39
12:00	25	8	19	55	38	43	33	19	4
13:00	2	27	36	79	151	26	23	18	23
14:00	20	110	2	99	50	83	1	5	30
15:00	24	60	18	90	37	18	31	27	9

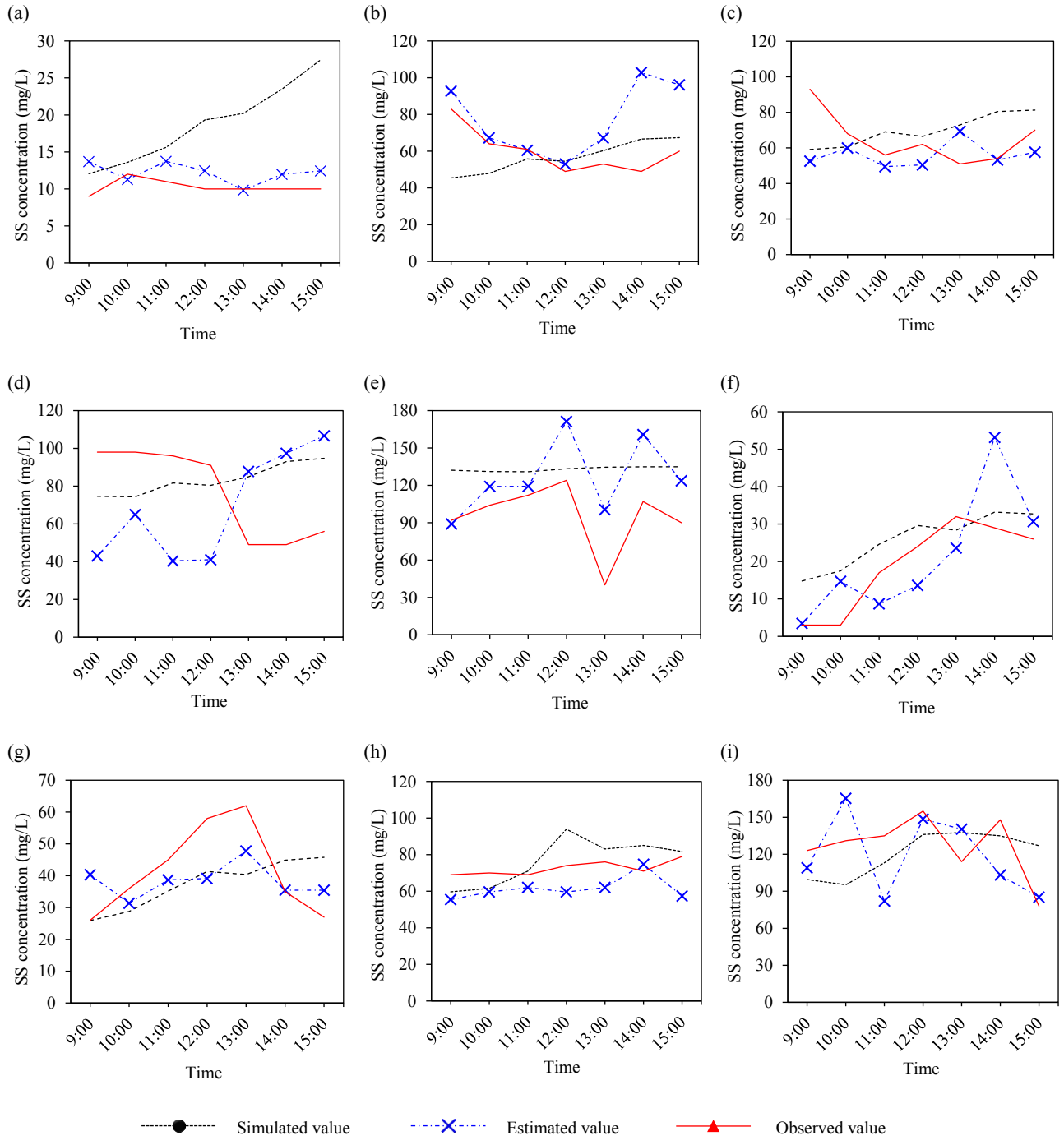

Figure 5. Changes in simulated values, estimated values, and observed values of SS concentration over time at point: a) A, b) B, c) C, d) D, e) E, f) F, g) G, h) H, and i) I

However, it was difficult to recognize the correlation of values from ODEM and UAV with observed values in Figure 5. Therefore, it was simply that their correlation with the observed values was expressed by the difference in concentration between them and the observed values, in which the concentration difference was taken absolutely. Table 7 highlights a number of p-values that differences in SS concentration have at each sampling point. It is known that if p-value is greater than or equal to 0.05 (significance level), there is no statistically significant difference in SS concentration between simulated values (SS1) and observed values (SS3), estimated values (SS2) and observed values (SS3). On the contrary, if p-value is less than 0.05, there is a statistically significant difference in SS concentration between SS1 and SS3, SS2 and SS3. In this regard, p-values at A and D, standing at 0.03 and 0.00,

respectively, were less than 0.05. Therefore, it is considered that statistically significant differences were seen at these two points. By comparison, there is no statistically significant difference in SS concentration between SS1 and SS3, SS2 and SS3 at the remaining points (B, C, E, F, G, H, and I). This declared clearly that although there was a big difference between the accuracy of ODEM and UAV (Figure S2), their results could accurately describe the observed values. In terms of considering correlation, Ganti (2019) argued that the correlation between the two variables was significant only if it had a value of greater than 0.8. Accordingly, the correlation of values from them with the observed values at different points was different, in which the correlation was distinctly shown at points F and D (Table 8). Consequently, it can be concluded that while a total of 9 points were observed, there were 2 points whose values described by ODEM and UAV were close to the observed values.

Table 7. Independent samples test of difference in SS concentration

Point	Difference	N	Mean	Std. deviation	Std. error mean	t	p-value
A	|SS1-SS3|	7	8.53	5.78	2.19	2.82	0.03
	|SS2-SS3|	7	2.17	1.47	0.56		
B	|SS1-SS3|	7	13.80	11.61	4.39	-0.41	**0.69**
	|SS2-SS3|	7	17.36	20.03	7.57		
C	|SS1-SS3|	7	16.93	10.76	4.07	0.46	**0.65**
	|SS2-SS3|	7	14.00	12.86	4.86		
D	|SS1-SS3|	7	27.24	12.66	4.79	-3.51	0.00
	|SS2-SS3|	7	47.36	8.38	3.17		
E	|SS1-SS3|	7	37.52	27.87	10.53	0.44	**0.67**
	|SS2-SS3|	7	31.47	23.28	8.80		
F	|SS1-SS3|	7	7.72	4.02	1.52	-0.63	**0.54**
	|SS2-SS3|	7	9.72	7.40	2.80		
G	|SS1-SS3|	7	12.02	7.47	2.82	0.65	**0.53**
	|SS2-SS3|	7	9.61	6.46	2.44		
H	|SS1-SS3|	7	9.06	6.27	2.37	-0.94	**0.36**
	|SS2-SS3|	7	12.11	5.80	2.19		
I	|SS1-SS3|	7	26.52	12.02	4.54	-0.01	**0.99**
	|SS2-SS3|	7	26.58	18.34	6.93		

SS1=Simulated SS, SS2=Estimated SS, SS3=Observed SS

The linear relationships between simulated values from ODEM and observed values, estimated values from UAV and observed values at all points are demonstrated in Figure 6. Detailed results of SS concentration from ODEM and UAV are provided in Table S4. The results in Table 8 showed that the correlation coefficients of simulated values with observed values and estimated values with observed values at most of the points were not too high (except for point F and D, respectively), especially at point A where the correlation coefficient of simulated values with observed values was not even greater than 0.1. That of estimated values with observed values, meanwhile, was found to be less than 0.1 at points A, B, C, and H. These denoted that both ODEM and UAV were not very good in concord with observed values in comparison with other studies. Typically, Dwinovantyo et al. (2017) reported that estimated SS concentration from ADCP closely correlated with that from field analysis. ADCP is a method of estimating SS concentration based on converting backscatter (echo) intensity measured from it into SS concentration using sonar equation. According to their study, ADCP could be used as a good technique in observing SS concentration, which was more comparatively viable than conventional method. As Shahzad et al. (2018) stated, results of SS concentration estimated by Landsat 7 and field analyses were not substantially different, and the Landsat 7 could be used as an effective means of daily water quality observation. Moreover, it was ascertained that high frequency observation with online auto sensors could be a coherent method of measuring SS presented by Valkama and Ruth

(2017). In our study, even though the linearity was quite low, the correlation coefficient for all points was not too low, as can be seen in Figure 6. Nevertheless, it was found that this was exactly dissimilar from results of suspended sediment concentration from the study by Thanh et al. (2017). The suspended sediment concentration simulated from Delft3D-4 model and Delft3D FM model proved to be in harmony with observed data (Thanh et al., 2017). On the other hand, if the accuracy between ODEM and UAV is taken into account, the ODEM showed its advantages in simulating the SS concentration and achieved more accurately than UAV because a correlation coefficient of simulated SS with observed SS was seen to be 0.8727 at point F which was greater than 0.8064 between estimated SS and observed SS at point D (Table 8). In addition, the correlation coefficient for all points between simulated SS and observed SS was also greater than that between estimated SS and observed SS (Figure 6).

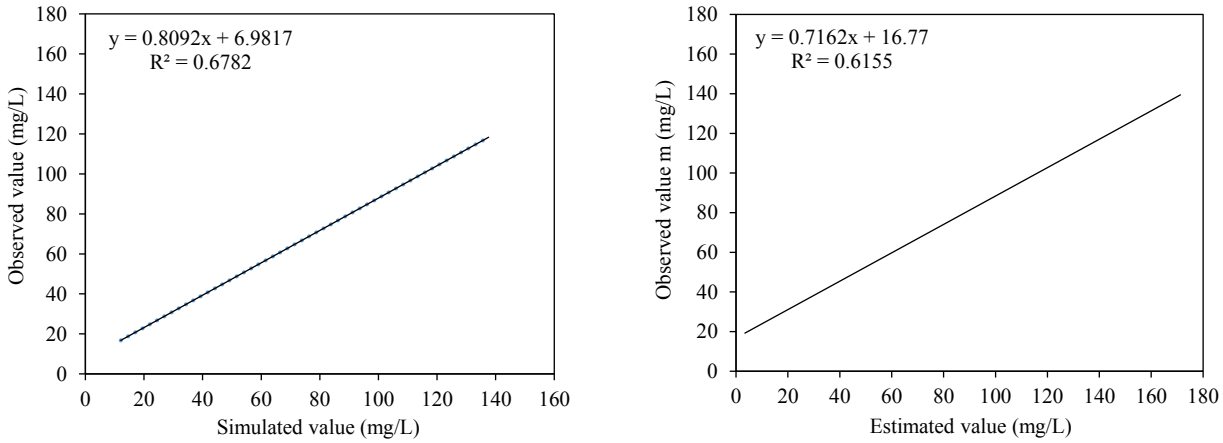

Figure 6. Linear relationship between simulated values and observed values, estimated values and observed values at all points

Table 8. Correlation of simulated values with observed values and estimated values with observed values

Point	Correlation coefficient with observed value		Correlation with observed value	
	Simulated value	Estimated value	Simulated value	Estimated value
A	0.0485	0.0536	Insig.	Insig.
B	0.4508	0.0650	Insig.	Insig.
C	0.2988	0.0691	Insig.	Insig.
D	0.7339	**0.8064**	Insig.	**Sig.**
E	0.1679	0.3992	Insig.	Insig.
F	**0.8727**	0.4329	**Sig.**	Insig.
G	0.3898	0.3898	Insig.	Insig.
H	0.3910	0.0261	Insig.	Insig.
I	0.1321	0.1321	Insig.	Insig.

Sig.=Significant, Insig.=Insignificant

4. CONCLUSIONS

The research into suspended solids has been carried out initially in this study to simulate the hydrodynamics of SS in Isahaya regulating reservoir as well as to review and evaluate simulation capability and accuracy of the ODEM model in comparison with UAV. As a result, the SS concentrations obtained from them were in relative accord with filed observed data. Therefore, this study has shown that the ODEM and UAV in the initial stage was quite good at monitoring SS concentration. As regards accuracy in monitoring SS, ODEM was better than UAV. Manipulation of the ODEM model was inexpensive, easy to operate and highly portable, which was very potential as an appropriate alternative for expensive observation of SS by manual methods. Apart from the favorable results achieved, some disadvantages remained. In this study, data were collected only once at each sampling point at each time. Some errors may have occurred, and the observed data may not have been fully representative of actual values of parameter concentrations observed at each sampling point during

the investigated time. Thus, future work should focus on multiple repetitions of sampling and analysis with long-term monitoring to bring about better results of hydrodynamic simulation SS concentration in the future.

ACKNOWLEDGEMENTS

The instruments and equipment in this study were supported by Department of Advanced Engineering, Nagasaki University. The most grateful thanks to Mr. Dohi for data from his study using UAV method for SS estimation and to all members in the laboratory of Water and Environmental Engineering, Nagasaki University for their cooperation during sampling process.

REFERENCES

Bilotta G, Brazier R. Understanding the influence of suspended solids on water quality and aquatic biota. Water Research 2008;42(12):2849-61.

Chebbo G, Bachoc A. Characterization of suspended solids in urban wet weather discharges. Water Science and Technology 1992;25(8):171-9.

Dwinovantyo A, Manik HM, Prartono T, Ilahude D. Estimation of suspended sediment concentration from Acoustic Doppler Current Profiler (Adcp) instrument: A case study of Lembeh Strait, North Sulawesi. IOP Conference Series: Earth and Environmental Science 2017;54(1):012082

Ganti A. Correlation coefficient [Internet]. 2019 [cited 2020 Jan 20] Available from: https://www.investopedia.com/terms/c/correlationcoefficient.asp.

Gartner JW. Estimating suspended solids concentrations from backscatter intensity measured by acoustic doppler current profiler in San Francisco Bay, California. Marine Geology 2004;211(3-4):169-87.

Harris DC. Quantitative Chemical Analysis. USA: Craig Bleyer; 2007.

Hodoki Y, Murakami T. Effects of tidal flat reclamation on sediment quality and hypoxia in Isahaya Bay. Aquatic Conservation: Marine and Freshwater Ecosystems 2006;16(6):555-67.

Kim S, Hayami Y, Tai A, Tada A. The Mechanism of bottom water variation in summer at the northern mouth of Isahaya Bay, Japan. Journal of Oceanography 2018;74(6):595-605.

Koga K, Vongthanasunthorn N, Araki H, Yamanishi H, Kawabe M, Ohwa N. Study on water quality analysis in the reservoir of Isahaya Bay land reclamation project. Environmental Engineering Research 2003;40:541-50.

Krawczyk D, Gonglewski N. Determining suspended solids using a spectrophotometer. Sewage and Industrial Wastes 1959;31(10):1159-64.

Li M-C, Liang S-X, Sun Z-C, Zhang G-Y. Optimal dynamic temporal-spatial parameter inversion methods for the marine integrated element water quality model using a data-driven neural network. Journal of Marine Science and Technology 2012;20(5):575-83.

Liang S, Nakatsuji K, Sun Z, Yamanaka R, Dalian P. Residual circulation system and its driving mechanism in the Bohai Sea. International Conference on Estuaries and Coasts; 2003 Nov 9-11; Hangzhou: China; 2003.

Liang S, Yamanaka R, Nakatsuji K. Typical seasonal circulation in the Bohai Sea. Proceedings of the Thirteenth (2003) International Offshore and Polar Engineering Conference; 2003 May 25-30; Honolulu, Hawaii: USA; 2003.

Magee MR, Wu CH. Response of water temperatures and stratification to changing climate in three lakes with different morphometry. Hydrology and Earth System Sciences 2017;21(12):6253-74.

Mitsugi Y, Vongthanasunthorn N, Mishima Y, Koga K, Araki H, Ittisukananth P. Long-term change of water quality in the reservoir of the Isahaya Bay reclamation project. Lowland Technology International 2013;15(1):21-8.

Murakami S, Tsujimoto T, Nakagawa H. Pick-up rate of sand and gravels. Japan Society of Civil Engineers 1992;(443):9-16.

Nagase S, Mishima Y, Mitsugi Y, Araki H, Yamanishi H, Koga K. Study on behavior of suspended solids under seawater in the reservoir of the Isahaya Bay reclamation project. Japan Society of Civil Engineers 2014;70(6): II_167-II_73.

Niki M, Nishida W, Noguchi M, Hashimoto A. Study on prediction and evaluation of water quality change in Isahaya regulating reservoir. Proceedings of Hydraulic Engineering 1999;43:1007-12.

Nishida W, Noguchi M, Yanamoto S. Prediction of the water quality change under a construction of sea dyke. Proceedings of Hydraulic Engineering 1997;41:457-62.

Nishida W, Suzuki S, Uehara Y, Shige R, Nozoe Y. Spatial and temporal changes of suspended solids in the northern waters of Isahaya Bay reclamation reservoir. Japan Society of Civil Engineers 2014;70(7):III_341-III_47.

Sasaki K. Changes in water quality of the regulating reservoir and impacts of Isahaya Bay reclamation project on Isahaya Bay and the Ariake Sea. Environment and Fisheries in the Ariake Sea 2017;4:13-5.

Schaeffer BA, Schaeffer KG, Keith D, Lunetta RS, Conmy R, Gould RW. Barriers to adopting satellite remote sensing for water quality management. International Journal of Remote Sensing 2013;34(21):7534-44.

Shahzad MI, Meraj M, Nazeer M, Zia I, Inam A, Mehmood K, Zafar H. Empirical estimation of suspended solids concentration in the indus delta region using Landsat-7 Etm+ imagery. Journal of Environmental Management 2018;209:254-61.

Tada A, Nakamura T, Sakai SI, Mizunuma M, Takenouchi K. Study on the characteristics of surface layer's currents around the mouth of Isahaya Bay. Coastal Environmental and Ecosystem Issues of the East China Sea 2010:13-27.

Thanh VQ, Reyns J, Wackerman C, Eidam EF, Roelvink D. Modelling suspended sediment dynamics on the subaqueous delta of the Mekong River. Continental Shelf Research 2017;147:213-30.

Valkama P, Ruth O. Impact of calculation method, sampling frequency and hysteresis on suspended solids and total phosphorus load estimations in cold climate. Hydrology Research 2017;48(6):1594-610.

Yamaguchi S, Hayami Y. Impact of Isahaya dike construction on concentration in the Ariake Sea. Journal of Oceanography 2018;74(6):565-86.